第 33 卷第 10 期 无 机 化 学 学 报 Vol.33 No.10
2017 年 10 月 CHINESE JOURNAL OF INORGANIC CHEMISTRY 1722-1730

一种用于活细胞中检测 Zn^{2+}的萘酚席夫碱类荧光探针

陈 邦 王少静 宋战科 郭 媛*
(西北大学化学与材料科学学院,合成与天然功能分子化学教育部重点实验室,西安 710127)

摘要:设计合成了 1 种基于 C=N 异构化和螯合荧光增强机理 (CHEF) 的 Zn^{2+}荧光探针 BMO 和 NBMO, 其结构经 ^{1}H NMR,^{13}C NMR,^{1}H-^{1}H COSY,HSQC,IR 和 HRMS 进行了表征。光谱分析实验结果显示,探针对 Zn^{2+}均具有较好的选择性和灵敏度,检出限分别为 30 和 21 nmol·L^{-1}。在 0~20 μmol·L^{-1} 浓度的范围内,BMO 和 NBMO 的荧光强度与 Zn^{2+}浓度可呈良好的线性关系。NBMO-Zn^{2+}配合物单晶结构和 Job 曲线证实该探针与 Zn^{2+}以 1:1 配位。NBMO 被成功应用于活细胞中 Zn^{2+}的检测。

关键词:荧光探针;C=N 异构化;螯合荧光增强;锌离子;活细胞成像
中图分类号:O626.23 **文献标识码**:A **文章编号**:1001-4861(2017)10-1722-09
DOI:10.11862/CJIC.2017.227

Naphthol-Based Shiff Base as a Selective Fluorescent Probe for Detecting Zn^{2+} in Living Cells

CHEN Bang WANG Shao-Jing SONG Zhan-Ke GUO Yuan*
(*Key Laboratory of Synthetic and Natural Functional Molecular Chemistry of Ministry of Education, College of Chemistry and Materials Science, Northwest University, Xi'an* 710127, *China*)

Abstract: Two fluorescent probes BMO and NBMO were developed for the highly selective detection of Zn^{2+} based on C=N isomerization and chelation-enhanced fluorescence (CHEF) mechanism. Structure identification of the probes was confirmed by ^{1}H NMR, ^{13}C NMR, ^{1}H-^{1}H COSY, HSQC, IR and HRMS spectroscopy. The results of spectral analysis show that BMO and NBMO are sensitive and highly selective to Zn^{2+}. The detection limit of BMO and NBMO are found to be 30 and 21 nmol·L^{-1} respectively. There is a good linear relationship between the fluorescence intensity of probes (BMO and NBMO) and the concentration of Zn^{2+} in the range of 0 to 20 μmol·L^{-1}. The X-ray crystal structure of the NBMO-Zn^{2+} complex exposes its coordination feature and the Job plots reveal a 1:1 probe-Zn^{2+} identification. The cell images show that NBMO can be used to detect intracellular Zn^{2+}.

Keywords: fluorescent probe; C=N isomerization; chelation-enhanced fluorescence; zinc ion; living cell imaging

Zn^{2+} is the second most abundant trace essential metals in the human body after iron and plays a critical role in many biochemical and physiological processes such as protein metabolism, reproduction, cell growth, cell division, cellular transport, immune system, and gene transcription[1-3]. Importantly, deficiency or excess of this essential trace element is known to have adverse consequences to human health[4]. Any disruption in the bio-availability of Zn^{2+} in the mammalian system may cause serious diseases such as Alzheimer′s, amyotrophic lateral sclerosis (ALS), Parkinson′s, ischemia, epilepsy[5], while excess accumula-

收稿日期:2017-05-23。收修改稿日期:2017-09-01。
国家自然科学基金(No.21472148,21072158),陕西省留学人员科技活动择优资助项目(No.20151190)和西北大学优秀青年学术骨干支持计划资助。
*通信联系人。E-mail:guoyuan@nwu.edu.cn

tion of Zn^{2+} in human body may lead to health hazards. Thus, spatiotemporal detection of Zn^{2+} in biological samples is of great significance for understanding the role of Zn^{2+} in biology.

Consequently, more and more researchers focus on the study of detection methods for Zn^{2+}. The topical detection methods include atomic absorption spectrometry (AAS)[6], atomic emission spectrometry (AES)[7], electrochemical method[8] and fluorescent sensors, wherein fluorescent probes have attracted enormous interest because of their high sensitivity, operational simplicity and instantaneous response[9-22]. Up to now, a number of fluorescent probes for detecting Zn^{2+} have been designed based on rhodamine[23], coumarin[24], quinolone[25], fluorescein[26] and BODIPY[27]. They have good binding affinity with Zn^{2+}. However, there still exists some drawbacks among the reported fluorescence probes, e.g. the detection limit of probes is restricted[28], some of the sensors are hard to synthesize[29], and optical properties are interfered from other metal ions, such as Cd^{2+} which exhibits highly similar chemical properties as Zn^{2+}[30]. Therefore, to develop the Zn^{2+} fluorescence probes with low detection limit, high selectivity and high sensitivity are expected to remain challenging.

Over the past few decades, various Zn^{2+} fluorescence probes have been designed and synthesized to address the above challenge, wherein the probes based on C=N isomerization mechanism have outstanding performance and attracted extensive attention. As we know, the fluorescence probe containing C=N double bond with a lone electron pair has good ability to coordinate with metal ions. Compounds with an unbridged C=N structure are often nonfluorescent due to the C=N isomerization. In contrast, complexation with metal ions restricts the rotation of the C=N bond and produces a chelation-enhanced fluorescence (CHEF) effect. Based on the mechanism, we report two novel Zn^{2+} fluorescence probes (BMO and NBMO) herein. Studies show that BMO and NBMO are highly selectivity for Zn^{2+} over its family Cd^{2+} and the other metal ions. The X-ray crystal structure of the NBMO-Zn^{2+} complex exposes its coordination feature and the Job plots reveal a 1∶1 probe-Zn^{2+} identification. Moreover, the cell images show that NBMO can be used to detect intracellular Zn^{2+}.

1 Experimental

1.1 Reagent and apparatus

Unless otherwise stated, all reagents were purchased from commercial suppliers and used without further purification. A549 cells were purchased from the Committee on type Culture Collection of Chinese Academy of Sciences. NMR spectra were collected on a Varian INOVA-400 spectrometer 400 MHz for ^{1}H NMR and 100 MHz for ^{13}C NMR. High-resolution mass spectra (HRMS) were obtained with an Ulti Mate 3000 Mass Spectrophotometer. FT-IR spectra were obtained in KBr pellets on a Bruker EQUIOX-55 FT-IR spectrometer. The single crystal structure was determined by a Bruker Smart ApexIICCD X-ray crystallography. Absorption spectra were recorded on a UV-1700 spectrophotometer. Fluorescent spectra were recorded on a Hitachi F-4500 fluorescence spectrophotometer. Cell imaging was observed under a confocal laser scanning microscope (Olympus FV1000) with excitation at 405 nm.

1.2 Sample preparation and measurements

Stock solutions (1 mmol·L^{-1}) of BMO and NBMO were prepared in DMSO. Stock solutions (10 mmol·L^{-1}) of the chloride salts of Cd^{2+}, Ca^{2+}, Mg^{2+}, Mn^{2+}, Hg^{2+}, Fe^{3+}, Al^{3+}, Cr^{3+}, Co^{2+}, Ni^{2+}, Cu^{2+} and Zn^{2+} metal ions and acetate salts of Pb^{2+} and Ag^{+} metal ions were prepared in fresh deionized water. The spectra changes of BMO and NBMO towards Zn^{2+} were evaluated in Tris-HCl buffer solution (10 mmol·L^{-1}, pH=7.4) containing 20% DMSO. Unless otherwise noted, for all the measurements, the excitation wavelength was at 376 nm, the excitation slit was at 10 nm, and the emission slit was at 10 nm.

1.3 Synthesis of BMO and NBMO

Synthesis of 1*H*-benzimidazole-2-methanamine (**1**): amino acetic acid (0.9 g, 12 mmol) and *o*-Phenylenediamine (1.08 g, 10 mmol) were dissolved in 6 mol·L^{-1} HCl (14 mL). The reaction mixture was stirred at 120 ℃ for two days. After being cooled to room

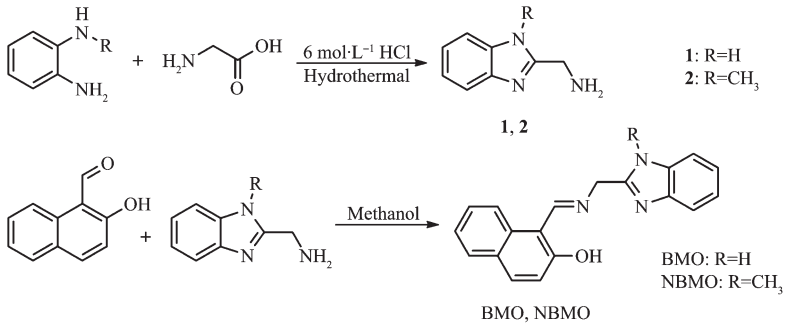

Scheme 1 Synthesis of BMO and NBMO

temperature, the pH of the reaction liquid was adjusted to 7~8 with strong aqua ammonia, then the mixture was frozen till the solid no longer formation. The solid was collected and recrystallized by distilled water to afford the desired product as colorless needle-like crystals. ^{1}H NMR (400 MHz, DMSO-d_6): δ 2.03 (br, 2H), 3.91 (s, 2H), 7.10~7.12 (m, 2H), 7.47~7.49 (m, 2H).

Synthesis of 1-methyl-1*H*-benzimidazole-2-methanamine (**2**): *N*-methyl-*o*-phenylenediamine (1.22 g, 10 mmol) and amino acetic acid (0.9 g, 12 mmol) were dissolved in 6 mol·L^{-1} HCl (14 mL). The reaction mixture was stirred at 120 ℃ for two days. After being cooled to room temperature, the pH of the reaction liquid was adjusted to 7~8 with strong aqua ammonia, then the mixture was frozen till the solid no longer formation. The solid was collected and recrystallized by distilled water to afford the desired product as light pink needle-like crystals. ^{1}H NMR (400 MHz, DMSO-d_6): δ 1.93 (br, 2H), 3.78 (s, 5H), 3.95 (s, 4H), 7.13~7.22 (m, 2H), 7.50 (d, *J*=7.8 Hz, 1H), 7.56 (d, *J*=7.7 Hz, 1H); ^{13}C NMR (100 MHz, DMSO-d_6): δ 161.31, 147.05, 141.24, 126.76, 126.27, 123.63, 114.86, 43.63, 34.62; HRMS (ESI): *m/z*, Calcd. for $C_9H_{11}N_3$[M+H]$^+$ 162.1031; Found 162.103 0.

Synthesis of BMO: 2-hydroxy-1-naphthaldehyde (0.86 g, 5 mmol) and compound **1** (0.88 g, 6 mmol) were dissolved in 15 mL anhydrous methanol. The reaction mixture was stirred at room temperature for 5 h. The precipitated was filtered, washed with cold methanol, and dried in vacuum to afford the desired product as a yellow solid. (1.38 g, yield: 92%). ^{1}H NMR (400 MHz, DMSO-d_6): δ 5.14 (s, 2H), 6.83 (d, *J*=9.1 Hz, 1H), 7.18~7.28 (m, 3H), 7.48~7.55 (m, 3H), 7.71 (d, *J*=7.5 Hz, 1H,), 7.81 (d, *J*=9.2 Hz, 1H), 8.17 (d, *J*=8.2 Hz, 1H), 9.42 (d, *J*=7.8 Hz, 1H,), 12.60 (s, 1H), 14.37 (s, 1H); ^{13}C NMR (100 MHz, DMSO-d_6): δ 174.50, 161.74, 151.28, 137.29, 134.33, 129.42, 128.44, 126.25, 124.50, 123.11, 122.74, 121.82, 119.39, 119.16, 111.82, 107.20, 50.83; FT-IR (KBr, cm^{-1}): 3 446, 3 014, 2 924, 2 739, 1 750, 1 629, 1 546, 1 432, 1 359, 1 319, 1 267, 1 190, 1 145, 1 032, 990, 837, 745, 621; HRMS (ESI): *m/z*, Calcd. for $C_{19}H_{15}N_3O$[M+H]$^+$ 302.129 3; Found 302.126 8.

Synthesis of NBMO: To a mixture 2-hydroxy-1-naphthaldehyde (0.86 g, 5 mmol) and compound **2** (0.97 g, 6 mmol) was added anhydrous methanol (15 mL). The mixture was stirred at room temperature for 5 h. The precipitated was filtered, washed with cold methanol, and dried in vacuum to afford the desired product as a yellow-green solid (1.46 g, yield: 94%). ^{1}H NMR (400 MHz, DMSO-d_6): δ 3.38 (s, 3H), 5.24 (s, 2H), 6.82 (d, *J*=8 Hz, 1H), 7.19~7.29 (m, 3H), 7.45~7.66 (m, 3H), 7.71 (d, *J*=7.8 Hz, 1H), 7.81 (d, *J*=9.3 Hz, 1H), 8.15 (d, *J*=8.3 Hz, 1H), 9.45 (d, *J*=8.1 Hz, 1H), 14.40 (s, 1H); ^{13}C NMR (100 MHz, DMSO-d_6): δ 174.63, 161.45, 151.35, 142.43, 137.31, 136.45, 134.30, 129.43, 128.48, 126.23, 124.56, 123.12, 122.72, 122.11, 119.30, 110.62, 107.18, 99.98, 49.09, 30.24; FT-IR (KBr, cm^{-1}): 3 677, 3 420, 3 029, 2 917, 1 622, 1 537, 1 466, 1 426, 1 398, 1 350, 1 313, 1 259, 1 188, 1 142, 1 060, 1 032, 995, 905, 844, 741; HRMS (ESI): *m/z*, Calcd. for $C_{20}H_{17}N_3O$[M+H]$^+$ 316.145 0; Found 316.143 0.

1.4 X-crystallographic analysis

Single crystals suitable for X-ray diffraction were prepared by slow evaporation of a solution of NBMO/$ZnCl_2$ in methanol at room temperature. The single

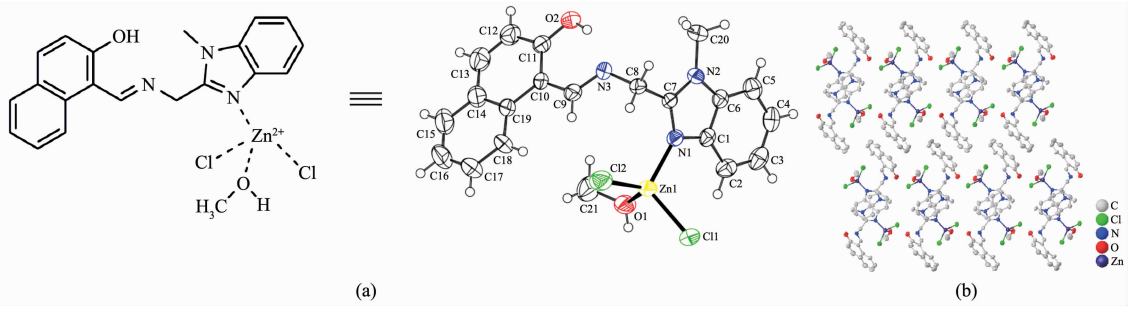

Fig.1　(a) X-ray crystal structures of NBMO-Zn^{2+} complex and (b) packing arrangement for NBMO-Zn^{2+}

crystal X-ray structure and packing diagram of the NBMO-Zn^{2+} complex are shown in Fig.1. NBMO and Zn^{2+} ion formed a 1:1 stoichiometry. Single-crystal X-ray diffraction data was collected on a Bruker Smart Ape II CCD X-ray diffractometer. The structure was solved by direct methods and refined by full matrix least-square on F^2 using the SHELXTL-97 program[31]. All non-hydrogen atoms were refined anisotropically. All the H atoms were positioned geometrically and refined using a riding model. The details of the crystal parameters, data collection, and refinements for complex NBMO-Zn^{2+} were listed in Table S1. Selected bond lengths and bond angles were listed in Table S2 and Table S3 respectively.

CCDC: 1558816.

1.5　Intracelluar Zn^{2+} imaging with NBMO

A549 cells were cultured in Roswell Park Memorial Institute 1640 (RPMI 1640) supplemented with 10% (*V*/*V*) fetal bovine serum (FBS), 100 units per mL of penicillin and 100 units per mL of streptomycin at 37 ℃ in a CO_2 incubator. The A549 cells were incubated with 20 μmol·L^{-1} of probe NBMO for 30 min at 37 ℃. Then pretreated with 60 μmol·L^{-1} Zn^{2+} for 30 min at 37 ℃ and after added with 1 μmol·L^{-1} TPEN (*N*,*N*,*N*′,*N*′-tetrakis(2-pyridylmethyl)-ethylenediamine) for 30 min at 37 ℃. The cells were washed three times with PBS buffer before cell fluorescence imaging experiments with confocal laser scanning microscopy[32].

2　Results and discussion

To get insight into fluorescence intensity changes with an increase of Zn^{2+} concentration, the fluorescence spectra changes of BMO and NBMO towards Zn^{2+} were evaluated. As shown in Fig.2, upon the addition of Zn^{2+} to the solution of BMO or NBMO, the emission intensity at 450 nm clearly increased. Moreover, there was a good linear relationship between the fluorescence intensity of probes (BMO and NBMO) and the concentration of Zn^{2+} in the range of 0 to 20 μmol·L^{-1}

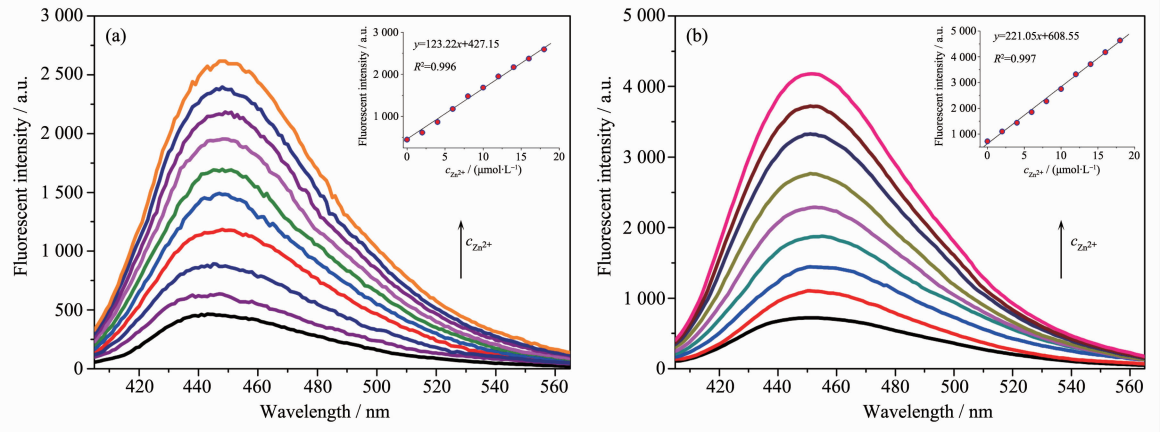

Insert figure: the linear relationships of (a) BMO and (b) NBMO towards Zn^{2+} (below 20 μmol·L^{-1})

Fig.2　Fluorescence changes of (a) BMO and (b) NBMO (20 μmol·L^{-1}) with different concentrations of Zn^{2+} (0~20 μmol·L^{-1}) in buffer solution with an excitation at 376 nm

(Inset in Fig.2). According to the reported definition (S/N=3), the detection limit of BMO and NBMO for Zn^{2+} were found to be 30 and 21 nmol·L^{-1} respectively. The results prove that NBMO has a higher sensitivity toward Zn^{2+} than BMO.

The binding constants K of BMO-Zn^{2+} and NBMO-Zn^{2+} were calculated by the Benesi-Hildebrand equation. Depending on the slope, the results obtained were $K_{BMO}=4.96\times10^4$ L·mol^{-1} and $K_{NBMO}=3.25\times10^4$ L·mol^{-1}, signifying that BMO and NBMO had a great binding affinity to Zn^{2+} (Fig.S17). In order to further study the binding of probes with Zn^{2+}, the Job plots were tested by using a total concentration of 20 μmol·L^{-1} probe and Zn^{2+}, and the results indicate that the combination of probes and Zn^{2+} is 1∶1 stoichiometry (Fig.3).

The kinetic studies were conducted by monitoring the fluorescence intensity changes of BMO and NBMO at 450 nm in the presence of Zn^{2+}. The results show that the chelation process can be completed within 30 s (Fig.4). The pH value of the system is often considered as a significant factor for the properties of fluorescent probe. The effect of pH on the fluorescence response of BMO and NBMO to Zn^{2+} ions was studied by adjusting the pH value ranging from 3.0 to 9.0. As shown in Fig.5, no noticeable fluorescence emission of pure BMO and NBMO were observed in a wide range of pH values. Upon the addition of Zn^{2+}, a significant increase in the fluorescence intensity were observed in the range of 4.0 to 9.0, which clearly indicated the compatibility of BMO and NBMO for biological applications under physiological conditions.

To further understand the fluorescent properties of BMO and NBMO with Zn^{2+}, the fluorescence response behavior of BMO and NBMO to various metal ions was systematically investigated (Fig.6). As expected, there were no obvious changes in the fluorescence intensity after adding other metal ions to BMO and NBMO solution, including Cd^{2+}, Ca^{2+}, Mg^{2+}, Pb^{2+}, Mn^{2+}, Hg^{2+}, Ag^{+}, Fe^{3+}, Al^{3+} and Cr^{3+}. However, the presence of Co^{2+}, Ni^{2+} and Cu^{2+} quench the fluorescence possibly because of the heavy metal effect. Moreover, the competitive experiments confirmed that the presence of metal ions, such as Cd^{2+}, Ca^{2+}, Mg^{2+}, Pb^{2+}, Mn^{2+}, Hg^{2+},

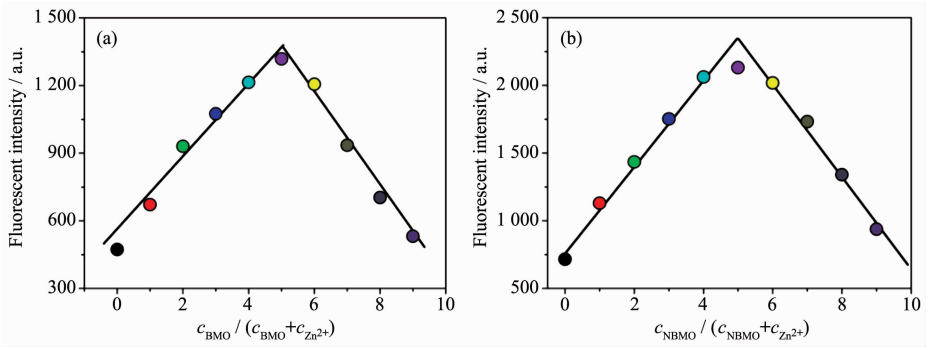

Total concentration of probe and Zn^{2+} were kept constant at 20 μmol·L^{-1}

Fig.3 Job plots of (a) BMO-Zn^{2+} and (b) NBMO-Zn^{2+}

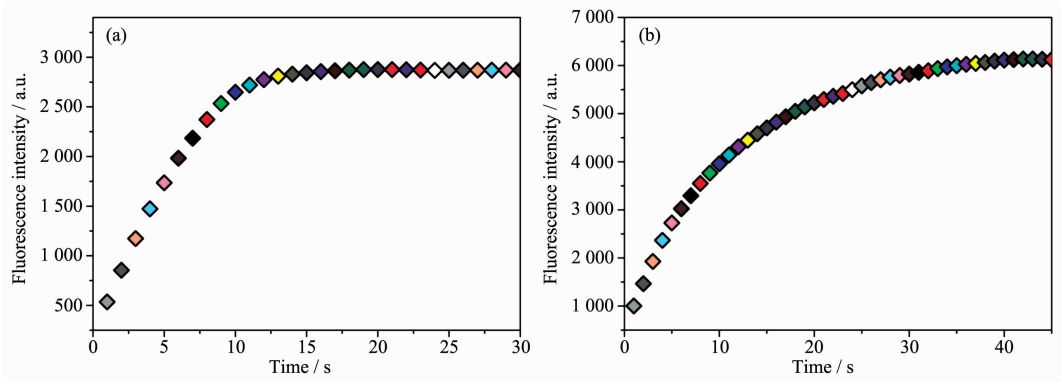

Fig.4 Time-course fluorescence response spectra of (a) BMO and (b) NBMO (20 μmol·L^{-1}) towards Zn^{2+} (60 μmol·L^{-1})

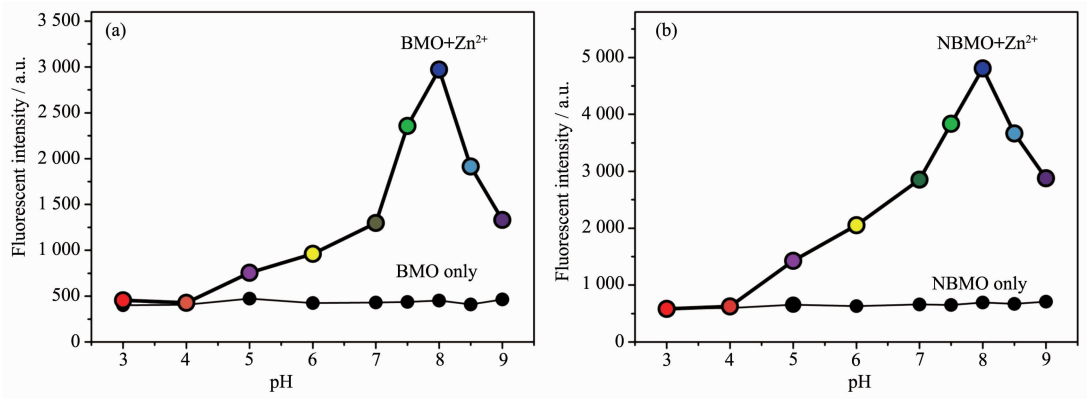

Fig.5　Effect of pH value on the fluorescence intensity of (a) BMO and (b) NBMO (20 μmol·L^{-1}) upon the addition of Zn^{2+} (20 μmol·L^{-1})

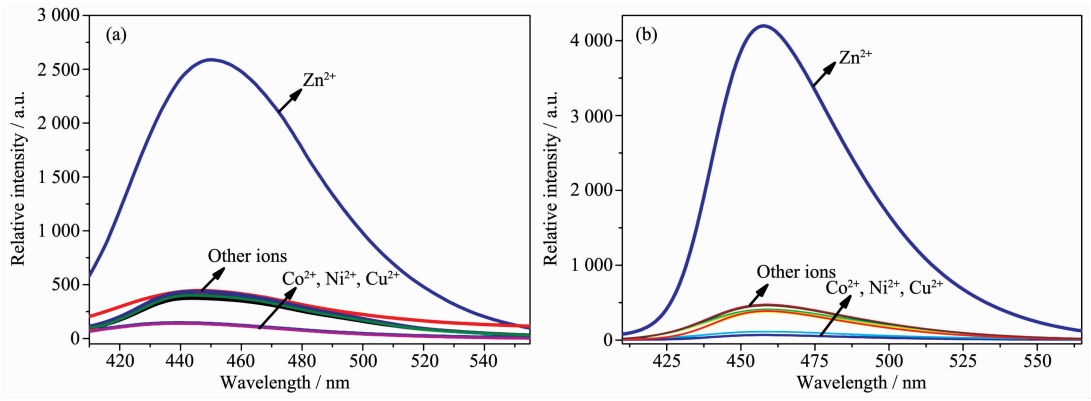

Concentration of Zn^{2+} was 20 μmol·L^{-1}; that of all the other metal ions was 40 μmol·L^{-1}

Fig.6　Fluorescence emission spectra of (a) BMO and (b) NBMO (20 μmol·L^{-1}) in the presence of different ions such as Cd^{2+}, Ca^{2+}, Mg^{2+}, Pb^{2+}, Mn^{2+}, Hg^{2+}, Ag^{+}, Fe^{3+}, Al^{3+}, Cr^{3+}, Co^{2+}, Ni^{2+}, Cu^{2+} and Zn^{2+} in Tris-HCl buffer (10 mmol·L^{-1}, pH=7.4)

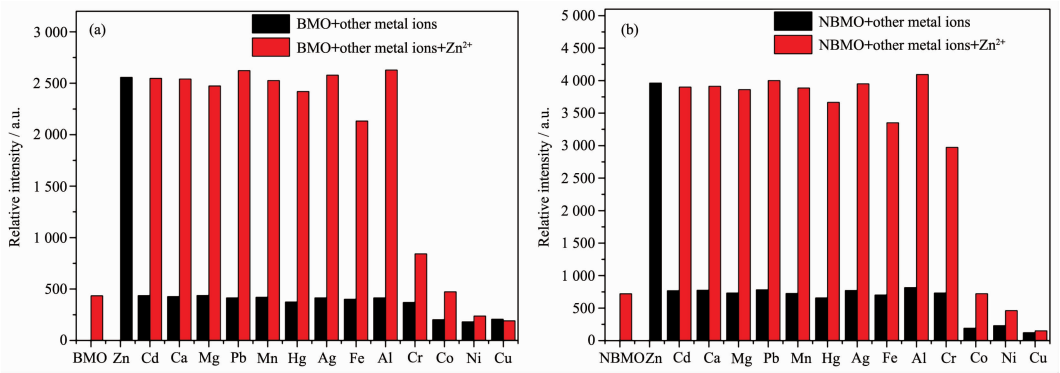

Fig.7　Metal ion selectivity of (a) BMO and (b) NBMO (20 μmol·L^{-1}) in Tris-HCl buffer (10 mmol·L^{-1}, pH=7.4); Concentration of Zn^{2+} was 20 μmol·L^{-1}, and that of the other metal ions 40 μmol·L^{-1}. Black bars represent the addition of the appropriate metal ions to the solution of BMO or NBMO. Red bars represent the subsequent addition of Zn^{2+} to the solution

Ag^{+}, Fe^{3+} and Al^{3+}, did not interfere with the enhanced fluorescence (Fig.7). However, the presence of Cr^{3+} would seriously weaken the enhanced fluorescence and Co^{2+}, Ni^{2+} and Cu^{2+} totally quenched the fluorescence, possibly because the complex formed between these metals and the probes was too stable to be replaced by Zn^{2+}. These results indicate that BMO and NBMO, have good selectivity toward Zn^{2+}, which facil-

itates the accurate detection under complex biosystem.

On the basis of the fluorescence response of BMO and NBMO toward Zn^{2+}, the recognition mechanism is proposed as shown in Fig.8. The weak fluorescence of BMO and NBMO are due to the free rotation around C=N bond. In contrast, complexation with Zn^{2+} inhibits the rotation of the C=N bond and produces a chelation-enhanced fluorescence (CHEF) effect. To confirm the supposed recognition mechanism, ^1H NMR titration experiment was carried out in DMSO-d_6/D_2O. Fig.9(a) shows ^1H NMR spectrum of NBMO. The peaks at 14.43 and 9.45 were assigned to -OH(H_a) and -CH=N-(H_b) of NBMO, respectively. Fig.9(b) shows the ^1H NMR spectra of NBMO upon the addition of Zn^{2+} with 3.0 equiv. concentrations. It was clearly found that the peak of H_a at 14.43 disappeared, demonstrating that -OH(H_a) was involvs in the complexation of Zn^{2+} and NBMO. The peak shape of -CH=N-(H_b) was changed from double peak to single peak after complexation, which further proved inhibition of the rotation of the C=N bond in the complex molecule. The ^1H NMR titration result supports the binding of Zn^{2+} with NBMO through a chelation reaction via phenolic -O atoms and the imine -N atoms.

The aforementioned favorable properties of BMO and NBMO in chemical system encouraged us to investigate their practical utilities in living cells. Taking into account the better spectral properties of NBMO, application of NBMO for cellular imaging was measured using A549 cells. Prior to being applied in cell imaging, MTT assay was first performed to assess its biocompatibility. Cytotoxicity experiments demonstrated minimal cytotoxicity of NBMO toward A549 cells at 25 $\mu mol \cdot L^{-1}$ (80% viability, Fig.S18). Next, we further investigated its potential utility for the detection of Zn^{2+} in living cells by using the confocal fluorescence microscope. As shown in Fig.10, the A549 cells displayed the weakly fluorescence after

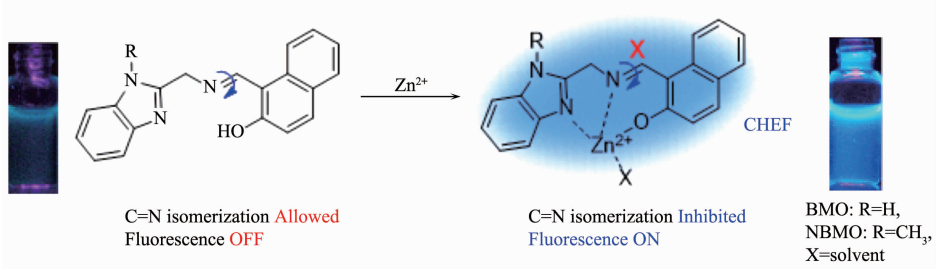

Fig.8 Recognition mechanism of BMO and NBMO to Zn^{2+}

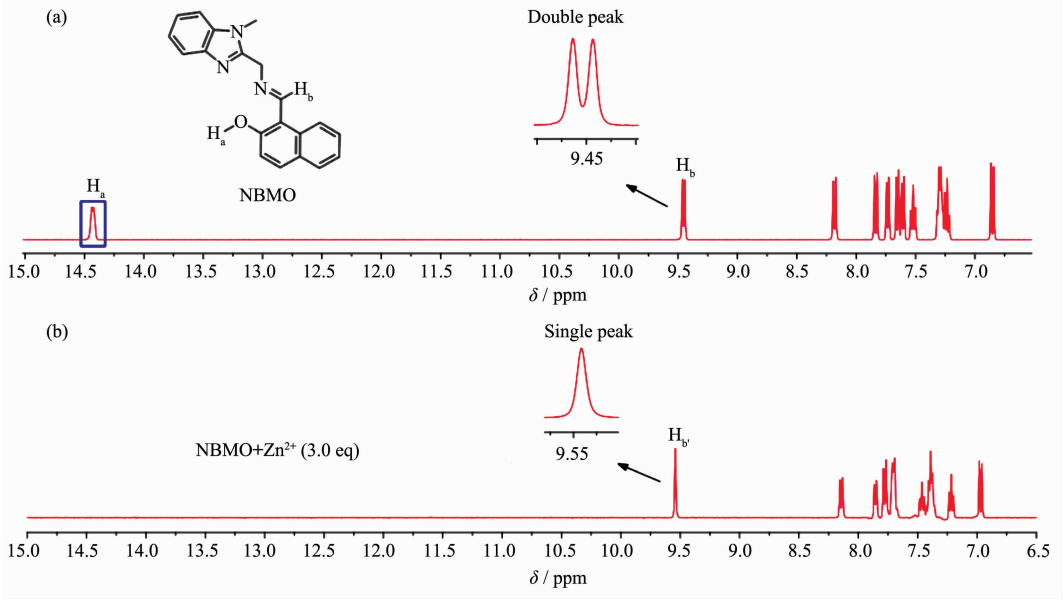

Fig.9 ^1H NMR spectra in DMSO-d_6 /D_2O of (a) NBMO only, (b) NBMO with 3.0 equiv. of Zn^{2+}

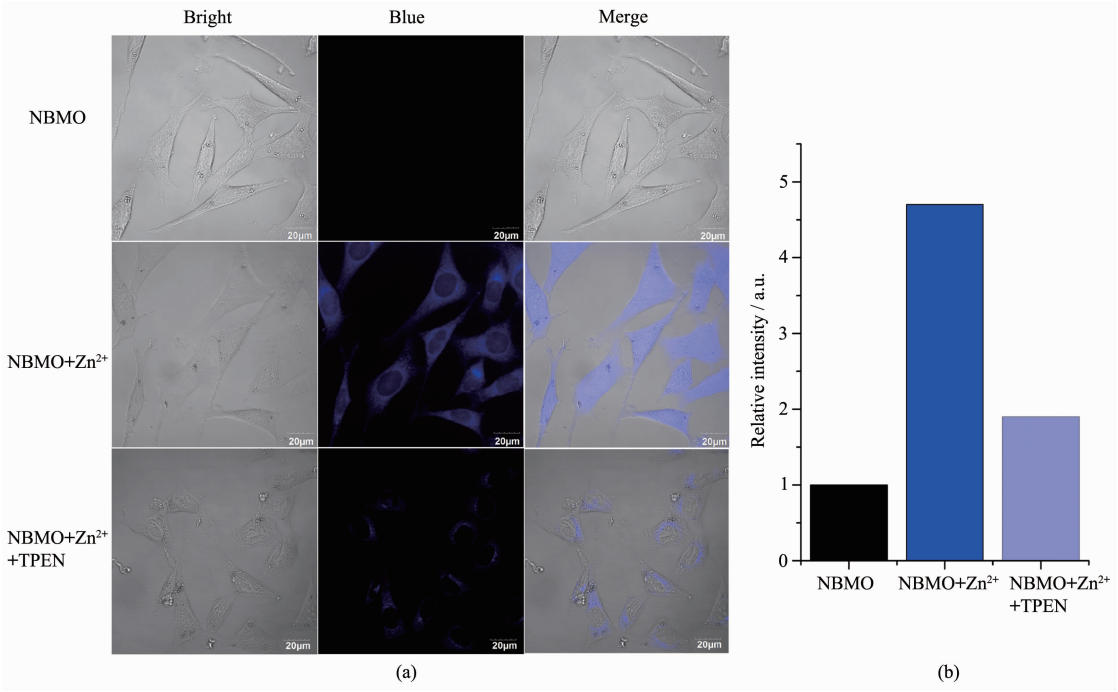

Pixel intensity from image row 1 is defined as 1.0; λ_{ex}=405 nm, λ_{em}=410~550 nm, scale bar=20 μm

Fig.10　(a) First row: Images of living A549 cells incubated with NBMO (20 μmol·L^{-1}) for 30 min; the second row: Images of living A549 cells incubated with NBMO (20 μmol·L^{-1}) for 30 min, and further incubated with Zn^{2+} (60 μmol·L^{-1}) for 10 min; the third row: Images of living A549 cells incubated with NBMO (20 μmol·L^{-1}) for 30 min, and further incubated with Zn^{2+}(60 μmol·L^{-1}) for 10 min, then incubated with TPEN (1 μmol·L^{-1}) for 10 min; (b) Relative pixel intensity of fluorescence images row 1, 2 and 3

incubated with the probe NBMO for 30 min at 37 ℃. After addition of Zn^{2+} for 10 min at 37 ℃, the fluorescence clearly increased, indicating that the NBMO could combine Zn^{2+} to form complex NBMO-Zn^{2+} and then enhance the fluore-scence intensity. After following addition TPEN for 10 min at 37 ℃, the strong fluorescence was decreased greatly. Thus, above results clearly document the applicability of NBMO as a fluorescent probe to detect intracellular Zn^{2+} ions.

3　Conclusions

We have successfully developed two novel probes, BMO and NBMO, as efficient chemical sensors for the highly selective detection of Zn^{2+} in aqueous media. Towards this aim, the two probes were designed and synthesized through a simple condensation of 2-aminomethylbenzimidazole derivatives and 2-hydroxy-1-naphthaldehyde based on C=N isomerization and chelation-enhanced fluorescence (CHEF) mechanism. Their kinetic study towards Zn^{2+} displayed a fast response time (both less than 30 s). Selective and competitive experiments were performed to exhibit an excellent selectivity of Zn^{2+} ions over its family Cd^{2+} and other metal ions. Moreover, the detection limit of BMO and NBMO were found to be 30 nmol·L^{-1} and 21 nmol·L^{-1} respectively, which exhibited an excellent sensitivity of the two probes. Meanwhile, NBMO has been used to image intracellular Zn^{2+} ions in living A549 cells with a good performance.

Supporting information is available at http://www.wjhxxb.cn

References:

[1] Bouain N, Shahzad Z, Rouached A, et al. *J. Exp. Bot.*, **2014**, **65**:5725-5741

[2] El-Hallag I S. *J. Chil. Chem. Soc.*, **2010**,**55**:67-73

[3] Frommer G, Vorbruggen G, Pasca G, et al. *EMBO J.*, **1996**, **15**:1642-1649

[4] WAN Dan-Dan(万丹丹), SU Guang-Yu(苏光余), XU Zi-Hua

(许子华), et al. *Chinese J. Inorg. Chem.*(无机化学学报), **2008**,**24**:1253-1260

[5] Chen J R, Teo K C. *Anal. Chim. Acta*, **2001**,**450**:215-222

[6] Monasterios C V, Jones A M, Salin E D, et al. *Anal. Chem.*, **1986**,**58**:780-785

[7] Oliveira P R D, Lamy-Mendes A C, Gogola J L, et al. *Electrochim. Acta*, **2015**,**151**:525-530

[8] Zhang L L, Zhu H K, Zhao C C, et al. *Chin. Chem. Lett.*, **2017**,**28**:218-221

[9] WANG Wei-Na(王维娜), ZHENG Yuan-Mei(郑元梅), CHEN Xue-Mei(陈雪梅). *Chinese J. Inorg. Chem.*(无机化学学报), **2014**,**30**:872-878

[10]Liu J, Lin Q, Yao H, et al. *Chin. Chem. Lett.*, **2014**,**25**:35-38

[11]WU Yu-Fang(吴玉防), CUI Ying-Na(崔颖娜), LI Shen-Min(李慎敏), et al. *Chinese J. Inorg. Chem.*(无机化学学报), **2012**,**28**:910-914

[12]Gan X P, Sun P, Li H, et al. *Biosens. Bioelectron.*, **2016**,**86**:393-397

[13]Liu H Y, Dong Y S, Zhang B B, et al. *Sens. Actuators, B*, **2016**,**234**:616-624

[14]Jia M Y, Wang Y, Liu Y, et al. *Biosens. Bioelectron.*, **2016**, **85**:515-521

[15]LIU Min(刘敏), TAN Hui-Long(谭慧龙), LIU Zhi-Guo(刘治国), et al. *Chin. J. Org. Chem.*(有机化学), **2013**,**33**:1655-1667

[16]Qin J C, Wang B D, Yang Z Y, et al. *Sens. Actuators, B*, **2016**,**224**:892-898

[17]Chen Y C, Bai Y, Han Z, et al. *Chem. Soc. Rev.*, **2015**,**44**:4517-4546

[18]Roy N, Nath S, Dutta A, et al. *RSC Adv.*, **2016**,**6**:63837-63847

[19]LI Chang-Wei(李长伟), YANG Dong(杨栋), YIN Bing(尹兵), et al. *Chin. J. Org. Chem.*(有机化学), **2016**,**36**:787-794

[20]Nie J, Li N, Ni Z H, et al. *Tetrahedron Lett.*, **2017**,**58**:1980-1984

[21]Zhu J L, Zhang Y H, Chen Y H, et al. *Tetrahedron Lett.*, **2017**,**58**:365-370

[22]ZHANG Chang-Li(张长丽), TIAN Jia-Jin(田佳津), SHAO Yang(邵阳), et al. *Chinese J. Inorg. Chem.*(无机化学学报), **2016**,**32**:2069-2074

[23]Erdemir S, Yuksekogul M, Karakurt S, et al. *Sens. Actuators, B*, **2017**,**241**:230-238

[24]Gao Y, Liu H M, Li P, et al. *Tetrahedron Lett.*, **2017**,**58**:2193-2198

[25]Ponnuvel K, Kumar M, Padmini V. *Sens. Actuators, B*, **2016**, **227**:242-247

[26]An J M, Yan M H, Yang Z Y, et al. *Dyes Pigm.*, **2013**,**99**:1-5

[27]Cao J, Zhao C C, Wang X Z, et al. *Chem. Commun.*, **2012**, **48**:9897-9899

[28]Ye J, Xiong J, Sun R C. *Carbohydr. Polym.*, **2012**,**88**:1420-1424

[29]Chen X Q, Pradhan T, Wang F, et al. *Chem. Rev.*, **2012**, **112**:1910-1956

[30]FAN Jiang-Li(樊江莉), XU Qun-Li(徐群利), ZHU Hao(朱浩), et al. *Chin. J. Org. Chem.*(有机化学), **2014**,**34**:1623-1629

[31]Sheldrick G M. *SHELX*-97, *Program for the Solution and the Refinement of Crystal Structures*, University of Göttingen, Germany, **1997**.

[32]QIU Lin(邱琳), JI Yi-Fan(季一凡), ZHU Cheng-Cheng(朱成成), et al. *Chinese J. Inorg. Chem.*(无机化学学报), **2014**, **30**:169-178